Computers & Geosciences 92 (2016) 79–89

Contents lists available at ScienceDirect

Computers & Geosciences

journal homepage: www.elsevier.com/locate/cageo

Research paper

A COMSOL–GEMS interface for modeling coupled reactive-transport geochemical processes

Vahid Jafari Azad [a], Chang Li [a], Circe Verba [b], Jason H. Ideker [a], O. Burkan Isgor [a,*]

[a] School of Civil and Construction Engineering, Oregon State University, Corvallis 97331, USA
[b] U.S. Department of Energy, National Energy Technology Laboratory, Albany 97321, USA

ARTICLE INFO

Article history:
Received 25 July 2015
Received in revised form
21 March 2016
Accepted 4 April 2016
Available online 8 April 2016

Keywords:
Reactive-transport modeling
(Geo)chemical modeling
Porous media
Finite element method
Multiphysics
GEMS

ABSTRACT

An interface was developed between COMSOL Multiphysics™ finite element analysis software and (geo) chemical modeling platform, GEMS, for the reactive-transport modeling of (geo)chemical processes in variably saturated porous media. The two standalone software packages are managed from the interface that uses a non-iterative operator splitting technique to couple the transport (COMSOL) and reaction (GEMS) processes. The interface allows modeling media with complex chemistry (e.g. cement) using GEMS thermodynamic database formats. Benchmark comparisons show that the developed interface can be used to predict a variety of reactive-transport processes accurately. The full functionality of the interface was demonstrated to model transport processes, governed by extended Nernst–Plank equation, in Class H Portland cement samples in high pressure and temperature autoclaves simulating systems that are used to store captured carbon dioxide (CO_2) in geological reservoirs.

1. Introduction

The modeling of coupled reactive-transport processes in porous media is important in several fields of geoscience, geoengineering, and materials science. These models are used to simulate and mitigate contaminate spills, design geothermal energy systems, model underground (bio)chemical processes, and predict service life of engineering materials (Bedient et al., 1994; Glasser et al., 2008; Voss, 1984). The sequestration of environmentally harmful gases in deep geological storage reservoirs has increased the importance of the application of these models to realistically predict the wellbore and cap-rock integrity in high temperature and pressure conditions (Johnson et al., 2004; Pruess et al., 2001; Xu et al., 2006).

The multi-phase and multi-component transport processes, coupled with complex chemical reactions, require integrated solution approaches that are computationally efficient and accurate. In general, there are two main approaches for such integrated models: (1) fully coupled models that incorporate chemical reactions within the solution algorithms of transport processes (Shen et al., 2013; Steefel and Lasaga, 1994) and (2) models that uncouple the chemical reactions from the transport equations within small time intervals (Huet et al., 2010; Kolditz et al., 2012; Xu et al., 2006). Both approaches can achieve accurate solutions with differences in computational expense. The latter method can be implemented using the operator splitting technique which simplifies the modeling of highly complex (geo)chemical systems and numerical scales. Operator splitting can also enhance the efficiency of the analyses and help prevent ill-conditioning problems (Nardi et al., 2014; Xu et al., 2006).

Operator splitting-based reactive-transport models typically rely on custom-designed reaction modules when simulating complex chemical behavior. These reaction modules are generally based on one of the two widely-used principles: the law of mass action (LMA) (Parkhurst and Appelo, 1999; Van der Lee, 1998; Westall et al., 1976) and the Gibbs Energy Minimization (GEM) (Eriksson et al., 1997; Kulik et al., 2013). GEM methods can manage an arbitrary number of phases in a variety of solutions (e.g. aqueous and non-aqueous fluids, gases, or solid solutions) to realistically simulate multi-component multiphase (geo)chemical systems (Kosakowski and Watanabe, 2014). Recent developments in LMA techniques have enabled them to be used in the analysis of multiphase systems as well (Leal et al., 2013).These approaches are able to model thermodynamic processes without assuming priori stable phases and are independent to mass balance constraints and defined redox states. (Kulik et al., 2013). The transport modules are typically based on finite difference methods (Steefel, 2009; Xu et al., 2006), finite volume methods (Shen et al., 2013) or finite element methods (Kolditz et al., 2012; Kulik et al., 2013; Nardi et al., 2014; Prevost, 1981; Wissmeier and Barry, 2009).

The coupling and parallelization of existing reaction and transport modeling codes for simulating multiphysics phenomena in porous media have received increased attention within the past

* Corresponding author.
E-mail address: burkan.isgor@oregonstate.edu (O.B. Isgor).

http://dx.doi.org/10.1016/j.cageo.2016.04.002
0098-3004/

decade (Kosakowski and Watanabe, 2014; Nardi et al., 2014; Wissmeier and Barry, 2009). Recently, the general purpose finite element software, COMSOL Multiphysics™ (Comsol, 2013), was connected to the LMA-based (geo)chemical calculation software PhreeqC (Parkhurst and Appelo, 1999). For this purpose two interfaces were developed: (1) a Matlab-based interface for modeling vadose zone processes (Wissmeier and Barry, 2009) and (2) a custom-designed interface (referred as iCP) using a Java Native Access (JNA) (Nardi et al., 2014). These developed interfaces allow the use of generic features of the finite element method (provided by COMSOL) and are efficient for large-scale three dimensional modeling.

In this paper, we present an interface that was developed to connect the GEM-based (geo)chemical modeling platform GEMS3K (Kulik et al., 2013; Paul Scherrer Institute, 2013; Wagner et al., 2012) to COMSOL API (Comsol, 2013) for the reactive-transport modeling of materials that are supported by the thermodynamic databases in GEMS. COMSOL (the transport module) is used to model multiphysics phenomena such as solute transport governed by Nernst–Planck equation for each aqueous chemical species (e.g. elemental or molecular ions, precipitated compounds), fluid flow, and heat transfer. (Geo)chemical calculations are performed by GEMS (the reaction module). These non-iterative operations are performed within a time-marching algorithm using an operator splitting method. The developed interface is able to consider a wide range of materials, temperatures and pressures, and can use special thermodynamic databases that have been implemented in GEMS formats such as CEMDATA (Heide, 1986; Hummel et al., 2002; Lothenbach et al., 2008; Lothenbach and Winnefeld, 2006; Matschei et al., 2007; Moschner et al., 2008). As an example, an application of the developed interface is demonstrated for modeling cement-based materials using the CEMDATA database at high temperature (from 0 °C to 100 °C) and high pressure ranges.

2. Theory

2.1. Transport module

The transport module, COMSOL Multiphysics™, uses the finite element method (FEM) to solve the coupled governing equations such as mass balance, fluid flow, and electro-neutrality. Critical components of some of these governing processes are briefly described in this section.

2.1.1. Mass balance

In this work, the mass balance equations are written for all chemical elements that exist in the analyzed system as:

$$\frac{\partial c_i}{\partial t}=\frac{\partial c_{s,i}+\varphi S_L c_{aq,i}+\varphi\left(1-S_L\right)c_{G,i}}{\partial t}=-\sum_{n_{DC}}\nabla\bullet J_{flow} \tag{1}$$

where n_{DC} is the number of chemical species and c_i is the concentration of individual atomic species from different solid ($c_{s,i}$); aqueous ($c_{aq,i}$) and gaseous ($c_{G,i}$) phases (mol/m^3 of sample); S_L is the saturation degree of the sample, which is obtained through the solution of fluid flow equation; φ is the porosity which changes as a function of time and space based on the changes in the solid phases; and J_{flow} (mol/(m^2 s)) is the flux of chemical species that include element c_i. As an approximation in the current research, the gas flow has been neglected, and the gaseous concentrations are obtained through the reaction equilibriums at each step. However, the presence of the gaseous phases was considered in the transport modeling of the elements in different phases.

The right hand side of Eq. (1) represents the summation of fluxes of all chemical species that include the specific chemical element with concentration c_i. The concentrations in different phases can be automatically obtained from the mole amounts of all chemical species and stoichiometry data from the reaction module. Because the solid, gaseous and liquid parts are not generally consistent in terms of units, the desired unit changes from reaction to transport module are handled in the interface. It should be noted that the species transport are generally very sensitive to porosity values. Therefore, it is important to have an accurate estimation of this term. The porosity function in Eq. (1) is calculated at each node of the domain as:

$$\varphi-\varphi_0=-\sum_j v_j\Delta n \tag{2}$$

where φ_0 is the initial porosity that is obtained from initial amounts of solid phases in the system; v_j (m^3/mol) is the molar volume for solid phase j; and Δn is the molar changes of solid phase at each time step when the solid phase amounts and the porosity field are updated.

In Eq. (1), the J_{flow} term which includes diffusion, electrical migration, chemical activity and advection, is obtained from Nernst–Planck equation for each aqueous chemical species as per:

$$J_{flow,i}=-D_i\nabla c_{aq,i}-D_i c_{aq,i}\frac{Fz_i}{RT}\nabla\phi-D_i c_{aq,i}\nabla\ln(\gamma_i)+c_i v_L \tag{3}$$

where D_i is the effective diffusion coefficient of each chemical species in porous media (m^2/s), F is the Faraday's constant (96,485 s A/mol), z_i is the charge of the species, R is the universal gas constant (8.314 J/°K mol), T is the absolute temperature (°K), ϕ is the electrical potential (V), γi is the chemical activity coefficient, and v_L is the liquid flow velocity (m/s). The reaction module, GEMS3K, is able to calculate the activities for high ionic strengths accurately from different activity models including Pitzer ion-interaction model (Pitzer, 1991) and Specific ion-interaction theory (SIT) (Ciavatta, 1980; Guggenheim and Turgeon, 1955).

To determine the effective diffusion coefficients of chemical species, the effects of porosity, tortuosity and temperature-dependent viscosity are considered. This coefficient can be approximated through empirical relations based on the diffusion coefficient in water (Mainguy et al., 2000) that is corrected for the effects of tortuosity and the saturation (Bary and Sellier, 2004; Shen et al., 2013) as follows:

$$D=2.9\times10^{-4}e^{9.95\varphi}\frac{k_B\tau}{6\pi\mu_L r}\times\frac{1}{1+625\left(1-S_L\right)^4} \tag{4}$$

where k_B is the Boltzmann content (1.38×10^{-23} m^2 kg/(s^2 K)), μ_L is the temperature-dependent liquid water viscosity, r is the chemical species radius, and τ is the tortuosity (Bažant and Najjar, 1972).

2.1.2. Fluid flow

The solute transport in porous media is highly sensitive to saturation. Richards's equation has been implemented in the transport module to account for the variability in saturation. Neglecting the mass transfer between fluid and solid phases, the fluid flow equations can be written as follows (Richards, 1931):

$$(\varphi-\varphi_r)\frac{\partial S_L}{\partial t}=\nabla v_L \tag{5}$$

where φ_r is the residual constant porosity; $(\varphi-\varphi_r)$ represents the available space for the transport of species; and v_L is the aqueous velocity that is obtained from Darcy's equation

(Boettcher et al., 2014):

$$v_L=\frac{k_{init}^{L}k_{rL}}{\mu_L}(\nabla P_L-\rho_L g\nabla h) \quad (6)$$

where $k_{init}{}^{L}$ is the permeability of water, which is the characteristic parameter of the porous medium; P (Pa), ρ (kg/m^3) and g (m/s^2) are the phase pressure, phase density and the acceleration of gravity, respectively; μ_L is the temperature-based liquid dynamic viscosity (Pa-s), which is determined from a dynamic viscosity at a reference temperature with empirical relations (Weast et al., 1985). Moreover, the permeability factors are updated with porosity based on Kozeny–Carman equation (Vangenuchten, 1980):

$$k = k_0\left(\frac{\varphi}{\varphi_0}\right)^3\left(\frac{1-\varphi_0}{1-\varphi}\right)^2 \quad (7)$$

where k and k_0 represent the current and initial permeability, respectively. In Eq. (6), k_{rL} is the relative permeability and approximated empirically through functions of saturation degree (Luckner et al., 1989; Vangenuchten, 1980):

$$k_{rL}=\sqrt{S_L}\left(1-\left(1-S_L{}^{1/\beta}\right)^{\beta}\right)^2 \quad (8)$$

where β is a material dependent coefficient that represents desorption or adsorption. For example, this parameter was obtained as 0.444 from a regression analysis for wellbore cement (Thiery, 2006). Finally, the flow pressure can also be simply approximated from the Van Genuchten model which is not detailed here for the sake of brevity (Van Genuchten, 1980).

2.1.3. Electro-neutrality

The principle of electro-neutrality forces the ionic species in the electrolyte solution to remain charge-balanced on a macroscopic scale. Because there is no external potential source, the charge balance equation should govern the system via:

$$\nabla i=\sum_j z_j\nabla\bullet J_{flow,j}=0 \quad (9)$$

where i is the ionic current (A). The electrical charges are obtained from stoichiometry data in reaction module (Shen et al., 2013).

2.2. Reaction module

The chemical processes are handled through the reaction module, GEMS3K (Kulik et al., 2013), which uses the GEM method (Kulik et al., 2013; Wagner et al., 2012) to solve for concentrations of chemical species, their activity coefficients, chemical potentials of chemical elements, and other thermodynamic quantities such as pH, fugacities and the redox state of the system (pe). GEMS3K can model heterogeneous aquatic (geo)chemical systems using numerous thermodynamic databases (Kulik, 2002; Kulik et al., 2013). In addition to the built-in databases, such as the SUPCRT92 (Johnson et al., 1992) and Nagra-PSI (Hummel et al., 2002) databases, there is a possibility to add other additional databases in the software's format such as CEMDATA database for cementitious systems (Lothenbach and Winnefeld, 2006). GEMS3K is the standalone variant of the GEM method without graphical user interface. The shared libraries of GEMS3K were linked to the developed interface to enable calling GEMS methods directly from Java interface (Kulik et al., 2004, 2013).

2.3. Kinetics of dissolution and precipitation

The kinetically-controlled minerals dissolve or precipitate because they are kept in disequilibrium with the rest of the equilibrated system. The existing empirical parameters for kinetic laws have many approximations and the dissolution rates are typically different from precipitation rates (Bethke, 1996). Because GEMS does not support kinetic calculations, dissolution and precipitation kinetics are handled through the interface itself and the dissolved (or precipitated) minerals are transferred to the reaction module. In the current version of developed interface, a kinetics module was designed to explicitly obtain the changes in solid phases. Because a non-iterative operator splitting method was used, the results are sensitive to time steps, and generally, the analysis required small time marching steps to avoid instability issues. (Leal et al., 2015). The general kinetics is briefly described here, but it is possible to define kinetics for other processes specific to cements (e.g. cement hydration), which is discussed further in numerical examples. A general form for multiple reaction mechanism, which is modified from Lasaga et al. (Lasaga, 1984; Palandri and Kharaka, 2004), is used in this work as:

$$\frac{dm}{dt}=-A\sum_i k_i(1-\Omega^{p_i})^{q_i} \quad (10)$$

where dm/dt (kg/s) is rate of mineral dissolution; A (m^2) is surface area; k_i (kg/m^2-s) is temperature-dependent rate constants following the Arrhenius relations; and Ω is mineral saturation index. Variability in values for constants, p_i and q_i, (assumed unity in this paper) is a source of uncertainty in the length of time to reach system equilibrium. The summation in Eq. (10) represents the inclusion of different mechanisms that may affect the rate law. In general, the most well-studied mechanisms are those in pure H_2O (neutral pH), and those catalyzed by H^+(acid) and OH^-(base). For many minerals, the full equation includes a term for each of these three mechanism via:

$$\frac{dm}{dt}=-A\left[k_{acid}\gamma_{H^+}{}^{n_1}(1-\Omega^{p_1})^{q_1}+k_{neutral}(1-\Omega^{p_2})^{q_2}+k_{base}\gamma_{H^+}{}^{n_3}(1-\Omega^{p_3})^{q_3}\right] \quad (11)$$

where k_{acid}, $k_{neutral}$ and k_{base} are the acid, neutral and base condition equilibrium constants and $\gamma_H{}^+$ is the hydrogen ion activity coefficient. Additionally, the precipitation rate data do not exist for most minerals, because of complexities in experiments due to undesired metastable mineral precipitations especially far from equilibrium at high degrees of super-saturation (Lasaga, 1984; Palandri and Kharaka, 2004). For the sake of simplicity, the dissolution and precipitation laws are assumed to be identical for all minerals if the precipitation parameters are not defined. The required parameters for Eq. (11) are taken from different references for the simplified rate equations (Lasaga, 1980, 1984; Steefel and Lasaga, 1994). After each step of transport modeling, performed in COMSOL, the resulted amounts of solid phases, as well as other required inputs (e.g. temperature), are transferred to the kinetics module that was developed in the interface. The kinetics module updates the amounts of dissolved solids that are accessible to the reaction module, GEMS. It is also possible to include kinetics in the transport module as well; however, in the current development, the kinetics was implemented in the interface to make it independent from the transport module for kinetic formulations that are differently formulated from Eq. (10) (e,g. cement hydration).

The developed interface is intended to be used to model simultaneous hydration and deteriorative processes of cement-based materials. Therefore, a brief discussion on the kinetics of cement hydration is provided here. A typical hydration of cement phases produces portlandite ($Ca(OH)_2$), calcium silicate hydrates (C–S–H)[1],

[1] C–S–H: Stoichiometry varies; a typical composition is 0.8–1.5 $CaO\cdot SiO_2\cdot$ 1.0–2.5 H_2O

Table 1
Phase analysis of class H cement used as input in the model[a].

Phase	C_3S	C_2S	C_3A	C_4AF	Na_2O	K_2O	MgO	SO_3	TiO_2	BaO	SrO	P_2O_5	Mn_2O_3	LOI
Wt (%)	65.71	11.33	0.17	13.64	0.12	0.15	2.72	2.81	0.21	0.07	0.11	0.14	0.06	0.79

[a] The cement chemistry notation for the main phases tri-calcium silicate or alite (C_2S), di-calcium silicate or belite (C_2S), tri-calcium aluminate (C_3A) and tetra-calcium aluminoferrite (C_4AF), where C=CaO; S=Si_2O_3; A=Al_2O_3; F=Fe_2O_3). LOI is loss of ignition.

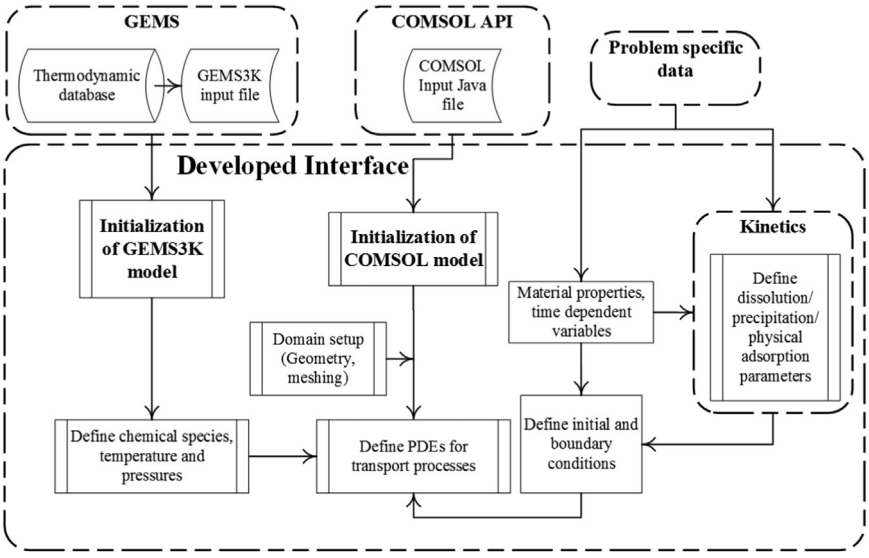

Fig. 1. Initialization of the system setup for modeling based on a defined problem definition in the interface.

ettringite (AFt)[2] and monosulfate (AFm)[3] phases. This process was simplified to take place via dissolution and precipitation processes (Lothenbach et al., 2008; Lothenbach and Winnefeld, 2006; Parrot and Killoh, 1984). The dissolution rate of the four important cement phases (C_3S, C_2S, C_3A and C_4AF (see Table 1)) determines the amount of calcium, aluminum, iron, silicon and hydroxide released into the solution at each step of the analysis. This approach determines the rate of the precipitation of different cement hydrated phases. In this regard, quantitative X-ray measurements have been used to derive empirical relationships for rate of hydration for a single phase compound as the minimum rate among: (1) nucleation and growth ($R_{1,\text{phase}}$), (2) diffusion ($R_{2,\text{phase}}$), and (3) shell formation ($R_{3,\text{phase}}$). The details of each part are omitted in this paper for brevity and can be found in (Lothenbach et al., 2008; Lothenbach and Winnefeld, 2006; Parrot and Killoh, 1984). The final rate of hydration degree is obtained based on the following relation:

$$R_{\text{phase}}=\min\{R_{1,\text{phase}},R_{2,\text{phase}},R_{3,\text{phase}}\}f_{w/c}\beta_{RH}\frac{A}{A_0}\exp\left(\frac{E_i}{R}\left(\frac{1}{T_0}-\frac{1}{T}\right)\right) \quad (12)$$

where A_o (m^2/kg) is the actual and reference surface area, A is the reference surface area (385 m^2/kg), T is the absolute temperature (°K), T_0 is the reference temperature (298.15 °K), and E_i is the activation energy (J), β_{RH} is the empirical parameter for the relative humidity (assumed 1 in this paper), and $f_{w/c}$ is the parameter for effects of water to cement ratio on the hydration rate. Finally, the overall hydration degree can be found as a weighted average for all phases.

3. COMSOL–GEMS interface architecture

An interface was developed to connect the GEM (geo)chemical modeling platform GEMS3K (GEMS open source kernel in C++) (Kulik et al., 2013; Paul Scherrer Institute, 2013; Wagner et al., 2012) to COMSOL API (the COMSOL Multiphysics™ Java interface) (Comsol, 2013) for the reactive-transport modeling of materials that are supported by the thermodynamic databases in GEMS. The COMSOL–GEMS interface is developed in Java where all COMSOL algorithms and data structures can be defined and used through COMSOL API. All C++ methods of GEMS3K are introduced to the Java interface through Java Native Interface (JNI). The shared libraries are produced based on the wrappers written in C++. An operator-splitting technique is used in this research to connect two modules together to minimize numerical instability problems like ill-conditioning. Fig. 1 illustrates the initial system setup algorithm in the developed interface. The interface initializes the GEMS3K model from the formatted GEMS input file and assigns the chemical speciation, temperature and pressure based on the defined conditions in the problem. The COMSOL Model object is also initiated in parallel, and the analysis domain and the partial differential equation (PDE) system are created within COMSOL directly through the developed interface. Due to the large number of chemical components in complex (geo)chemical systems, the interface gets the list of chemical elements and produces all transport equations automatically in a string format and passes them to COMSOL API. In addition, the general variables including the temperature based diffusion coefficients (see Eq. (4)), electrical

[2] AFt: $3CaO\cdot Al_2O_3\cdot 3CaSO_4\cdot 32H_2O$
[3] AFm: $3CaO\cdot Al_2O_3\cdot CaSO_4\cdot 12H_2O$

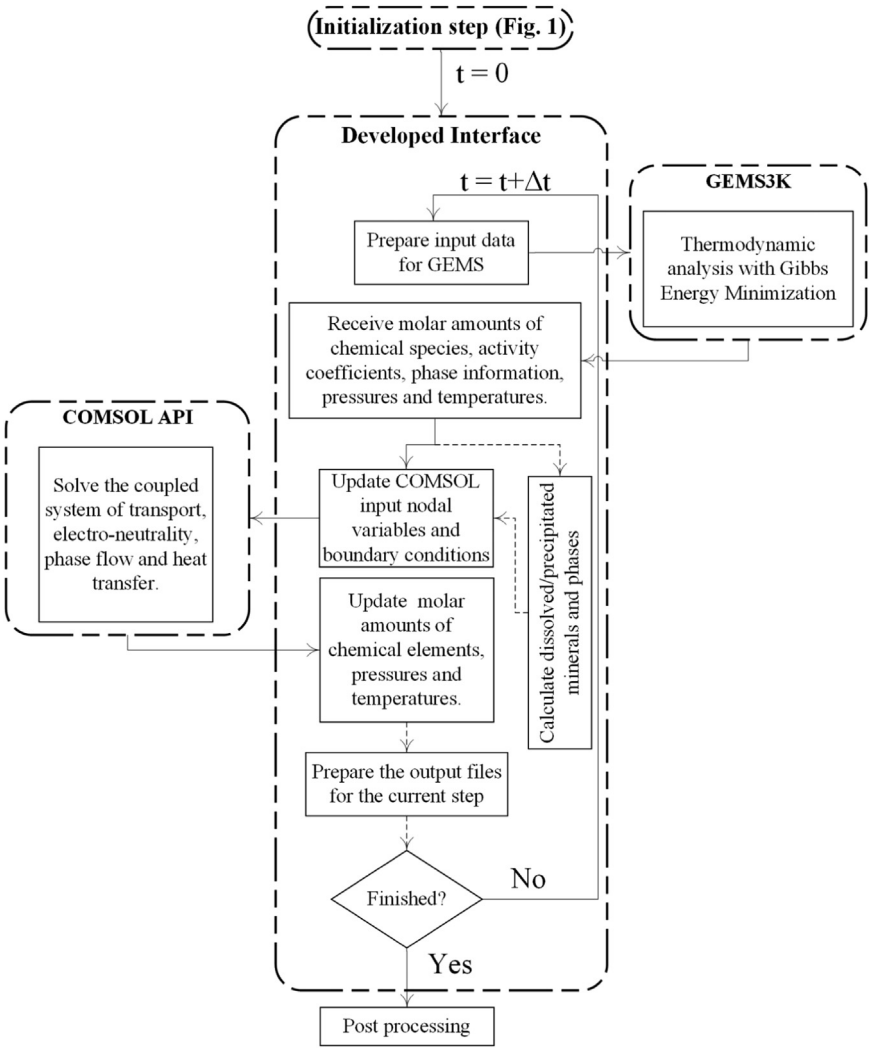

Fig. 2. Time-marching algorithm managed by the developed COMSOL–GEMS interface.

charges and temperature vectors are provided by the interface. Other chemical variables such as activities are obtained from the GEMS3K module in each step. The transport module, COMSOL, is responsible for all modeling steps, including geometry definition and automatic meshing of the domain.

Fig. 2 illustrates schematically the operator splitting solution process within a time-marching algorithm. When all data structures are defined in COMSOL and GEMS3K, the chemical setup is given to GEMS3K to find the equilibrium state for the case. Next, the resulted data are added to the interface computations on dissolution kinetics. The dissolution mole amounts are treated as source terms in transport equations in the transport module, COMSOL. However, for some cases where an incremental form is used for dissolution and precipitation kinetics (see example 3 for cement-based materials), it is preferred to handle the kinetics in the interface, as discussed earlier, and update the final values for the transport module, as initial conditions. Chemical speciation (including dissolved solid phases) is first transferred to GEMS and the equilibrated results are then given to COMSOL as initial conditions for the next step. This procedure always keeps the chemical species in equilibrium without the need for iterations.

After the initial conditions and equation parameters (e.g. temperature-based diffusion coefficients, permeability and dynamic viscosities) are updated in the interface, the transport equations are solved for the time step. For this, all data are transferred to the transport module and the fully coupled transport equations are solved: each step of transport modeling couples the transport and fluid flow equations; therefore, this step results in changes in the chemical element amounts, temperature and pressure vectors at each finite element node of the domain. Next, these data are transferred back to the interface. The process is repeated for the desired duration of the analysis.

Because a non-iterative operative-splitting method is used, the interface is used to manage GEMS3K for its convergence parameters when convergence issues arise during thermodynamic calculations. A GEMS Smart Initial Approximation (SIA) was setup in the interface that uses the previous equilibrated chemicals to obtain the current chemical speciation. However, in cases where convergence issues may arise (due to high dissolution rates, high pressure or high temperature gradients), the computation method switches to another GEMS algorithm, Automatic Initial Approximation (AIA). Generally, SIA required about 10–20 iterations while AIA might need more than 300 iterations to converge. Moreover, COMSOL uses the main indicators for the oscillatory results (i.e., Peclet and Courant numbers) to check the effects of high gradients where advection-based transport adds hyperbolic parts to partial differential equations. The interface overcomes this problem using COMSOL's flux corrected transport algorithms.

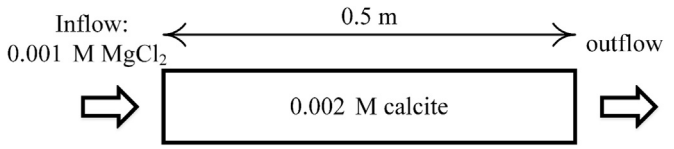

Fig. 3. The 1D domain for the benchmark problem. Temperature and pressure are assumed as 25 °C and 1 bar.

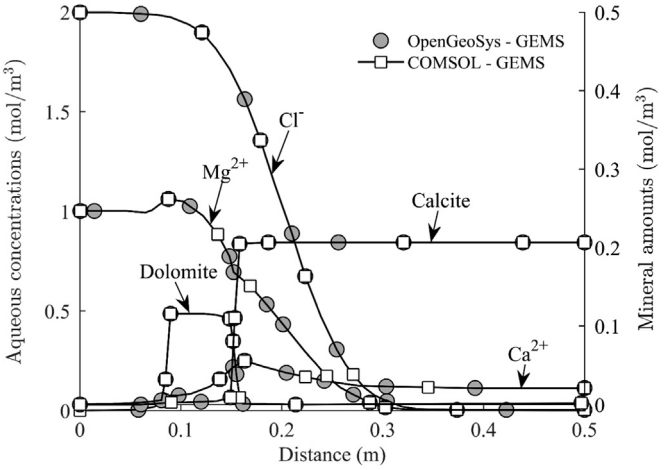

Fig. 4. Benchmark comparisons with OpenGeoSys-Gems.

4. Numerical examples

4.1. Benchmark example #1

The benchmark example presented here by Engesgaard and Kipp (1992) was used by a number of researchers for testing the reactive-transport modeling developments (Kulik et al., 2013; Shao et al., 2009). Fig. 3 illustrates the domain geometry, where a continuous water flow with dissolved magnesium chloride (with a concentration of 1×10^{-3} M) is infiltrated into a one-dimensional 0.5 M column of calcite with a velocity of 9.375×10^{-6} m/s. the porosity is assumed 0.32 while the pore solution inside the column is also assumed as calcite saturated (with a concentration of 2×10^{-3} M). the dispersion length (α_L), is also considered as 0.0067 m.

For the current modeling, some features of the interface including the dissolution kinetics, parameter calculation (e.g. diffusion coefficients), fluid flow and porosity change are not applied. The results of the model are compared to the predictions of the existing coupled reactive-transport platform, OpenGeoSys-Gems interface (Kosakowski and Watanabe, 2014). While the main transport mechanism is advection, the diffusivity was also considered in this example. The 1-D domain was divided equally into 50 finite elements. The temporal discretization is managed automatically by the transport module (i.e. COMSOL) based on the convergence rates of each system. However, the output time intervals can be customized, and in the current example, the results are presented at every 100 s.

Fig. 4 compares the concentration profiles after 21,000 s of simulation for chloride (Cl^-), magnesium ion (Mg^{2+}), calcium ion (Ca^{2+}), calcite, and dolomite predicted by the COMSOL–GEMS and OpenGeoSys-GEMS platforms. The dominant process in this problem is advection which causes the calcite temporary dissolution and dolomite precipitation in the column.

As shown in Fig. 4, the results from COMSOL–GEMS match to those of OpenGeoSys-GEMS predictions. These plots are also consistent with OpenGeoSys-PhreeqC and OpenGeoSys-ChemApp

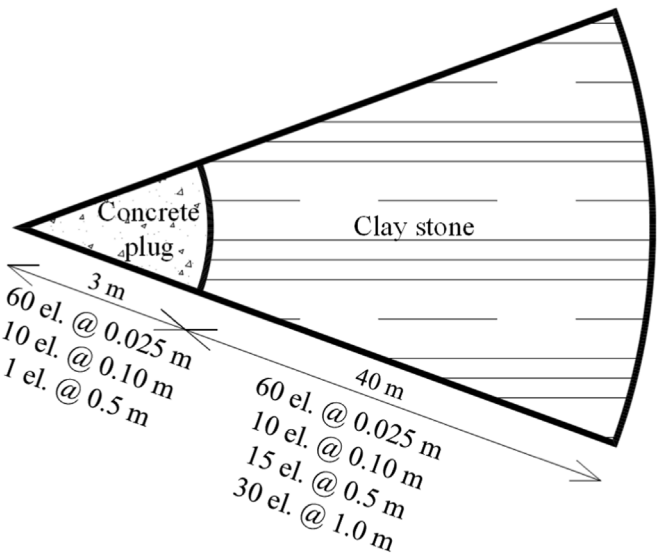

Fig. 5. The modeled system for the benchmark example #2.

interfaces which use other methods for calculating equilibria (Kulik et al., 2013; Shao et al., 2009). For the clarity of Fig. 4, these results are not shown. Although the use of an open-source software as the transport module has its merits, there are also many advantages of using a generic finite element software (e.g. COMSOL) such as (1) the ease of including any additional coupled multiphysics phenomena to the problem (e.g. heat transfer); (2) the access to inherent mesh generation/refinement and nonlinear solution algorithms; and (3) the possibility to use the post-processing features.

4.2. Benchmark example #2

The goal of this example was the benchmarking of the developed COMSOL–GEMS interface with a chemically complex benchmark example that includes porosity change and complex chemical thermodynamic process. This example compares the results from the developed interface with a code benchmark by Marty et al. (2015a) for a nuclear waste reactive transport model. The example was recommended for benchmarking codes that model complex (geo)chemical systems. Marty et al. simulated the cement/clay interface with a complex chemistry using several codes; i.e., TOUGHREACT (Xu et al., 2011, 2006), PHREEQC (Parkhurst and Appelo, 1999), CRUNCH (Steefel, 2009; Steefel and Yabusaki, 1996), HYTEC (Van Der Lee et al., 2002, 2003; Van der Lee and Lagneau, 2004), ORCHESTRA (Meeussen, 2003) and MIN3P-THCm (Mayer et al., 2002)). The main purpose of their study was to increase the confidence of safety analysis in both waste management and CO_2 storage. The model included a concrete plug surrounded by clay stone with low permeability (Callovian-Oxfordian claystone, CO*x*) as shown in Fig. 5. The current example compares the element results of *CASE 3* of the benchmark with fast kinetics. For clarity of presentation, the results of the developed GEMS-COMSOL interface were compared the results of HYTEC simulations since simulation results from other codes (e.g. THOUGHREACT, CRUNCH, etc.) were similar to each other and those of HYTEC. Since our goal was to provide a benchmark comparison to demonstrate the GEMS-COMSOL interface, we used the assumptions stated in this specific benchmark example, which includes diffusion-driven transport with constant diffusion coefficients and without porosity coupling. Although our model is designed to solve more complex systems that are governed by the Nernst-Plank equation with variable transport properties and

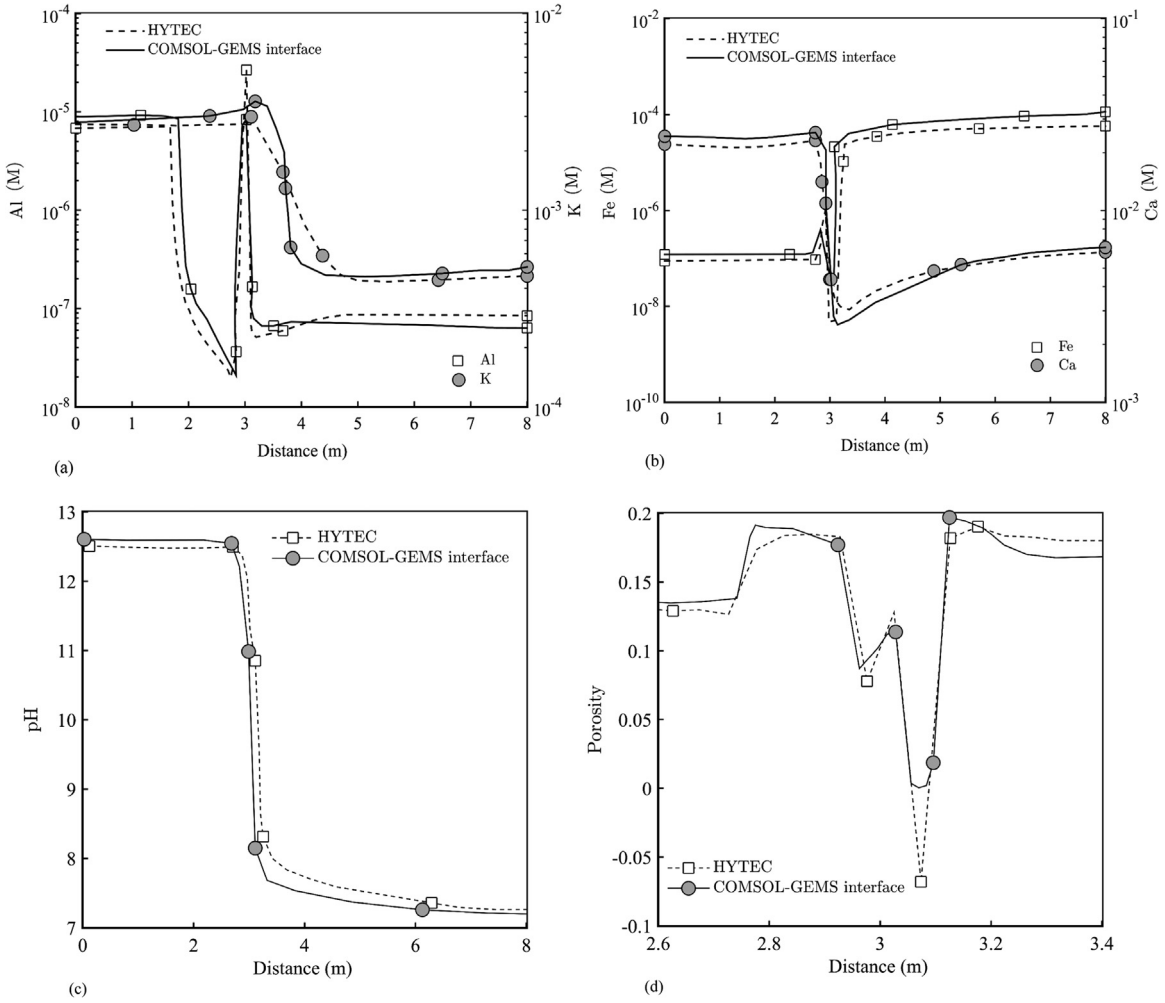

Fig. 6. Comparison of the selected results from the proposed COMSOL–GEMS interface and results from the reactive transport modeling by HYTEC (Marty et al., 2015a) after 10,000 years of interaction: (a) Al–K, (b) Fe–Ca, (c) pH and (d) porosity.

porosity coupling, it can also simulate Fickian processes by making the necessary assumptions on model parameters.

Fig. 5 shows the modeled geometry that included a 3-m radius concrete core surrounded by a 40-m radius of clay stone. The concrete was considered to be fully hydrated, and isothermal conditions (T=25°C) were assumed. The mineralogical and chemical characteristics of concrete and CO*x* are described in detail by Marty et al. (2015a). GEMS thermodynamic databases (CEMDATA and Nagra PS) were used as the base for the current model (Hummel et al., 2002). The investigated phases in the benchmark example that were not included in the GEMS databases were added to GEMS input file; these phases included Chlorite (Cca-2), Illite (IMt-2), Microcline and Montmorillonite (HcCa). The effective diffusion coefficients were assumed constant as 2.6×10^{-11} m^2/s for claystone and 9×10^{-12} m^2/s for concrete. Moreover, the porosities for claystone and concrete were taken as 18% and 13%, respectively. As shown on Fig. 5, the discretization was refined to 0.025 Lagrangian elements for 1.5 m across the cement/clay interface, to capture the large gradients. The kinetics of dissolution and precipitations were considered based on Marty et al. (2015b, 2014) and are not mentioned here for the sake of brevity.

Comparisons between the developed interface and the benchmark results are provided in Fig. 6. In general, the mineralogical transformations resulted from the proposed interface demonstrated consistent results with those of the reference benchmark. Although they are not shown here for brevity, the analysis confirmed the predictions of the benchmark example that indicated the dissolution of the solid phases in concrete (C–S–H, portlandite, C_3FH_6 and monocarboaluminate ($Ca_4Al_2CO_9$:10.68H_2O)) and clay (smectite, quartz and dolomite). Additionally, calcite, saponite and clinoptilolite (Ca) ($Ca_{0.55}(Si_{4.9}Al_{1.1})O_{12}$:3.9$H_2O$) were observed in clay. Finally, the amount of C–S–H (Tobermorite I and II) increased, and ettringite, saponite and ferrihydrate were precipitated. Fig. 6a and b provides the comparisons of four element concentrations (i.e. Fe, Ca, Al and K) along the central axis of the radial domain. The results for other elements are very close to those in the benchmark example; hence, they are not shown here for brevity. A similar trend for solid phases was also obtained with small discrepancies due to kinetics application in the code. Predictions for the pH were similar as shown in Fig. 6c. The differences from the proposed interface results and the benchmark example likely arise from (1) small differences in database, (2) difference in the kinetic implementations, and (3) differences in activity models. Additionally, the minimum porosity was set to zero in the current development which lead to some differences in the negative porosity regions of the benchmark example (Fig. 6d).

4.3. Reactive-transport modeling of CO_2 sequestration in wellbore cement

Storing captured carbon dioxide (CO_2) in geological reservoirs is a method to mitigate climate change. Studies show that the well

Table 2
Chemical composition of synthetic Mt. Simon Brine which is used as the initial boundary condition in the model.

Phase	NaCl	$CaCl_2$	$MgCl_2$	Na_2SO_4	$NaHCO_3$
Weight (mol/m^3)	1015.74	16.981	60.00	20.00	10.00

Table 3
Kinetic constants for rate law at 25 °C. The unfilled parameters in the table show that the dissolution is not sensitive to the process.

Mineral		k_i^{25C} (mol/m^2-s)	E_j (kJ/mol)	n	A (m^2/g)
portlandite	Neutral	2.18×10^{-08}	74.9	0.600	0.154
	Acid	8.04×10^{-04}			
C–S–H (1.6)	Neutral	1.60×10^{-18}	-	0.275	2.000
	Acid	5.94×10^{-08}			
Katoite	Neutral	1.60×10^{-18}	-	0.275	0.057
	Acid	5.94×10^{-08}			
Hydrotalcite	Neutral	1.60×10^{-18}	-	0.275	0.100
	Acid	5.94×10^{-08}			
Ettringite	Neutral	1.14×10^{-12}	-	-	0.098
	Acid	8.04×10^{-7}			
Calcite	Neutral	1.55×10^{-06}	23.5	-	0.026
	Acid	5.00×10^{-01}	14.4	1.000	
	Base	6.55×10^{-03}	56.1	1.982	
Magnesite	Neutral	4.47×10^{-10}	63.0	-	0.026
	Acid	4.37×10^{-05}	19.0	-	

cement in high pressure and temperature underground conditions is vulnerable to deterioration during carbon storage where resulting CO_2 leakage pathways could occur (Gasda et al., 2004). Use of an accurate and efficient numerical model can quantify the rate of degradation which could have implications in CO_2 sequestration process and its safety.

The developed COMSOL–GEMS interface was used to model such a scenario and to compare the results of an experimental study on Class H Portland cement samples in high pressure and temperature autoclaves simulating downhole conditions (Ideker et al., 2014). Class H cement is typically used for constructing and/or filling oil wellbores (new or abandoned). The chemical analysis of the unhydrated cement, which was used in the experimental setup (Ideker et al., 2014), is provided in Table 1. Cement prisms were prepared with a water-to-cement ratio (w/c) of 0.38 and cured for 28 days in a synthetic brine (Mt. Simon brine from the Illinois Basin) as shown in Table 2. The details of the experimental setup and procedures are presented by Ideker et al. (2014).

It was assumed that brine was fully saturated with CO_2, a state obtained through a trial and error method in the reaction module and changed with temperature and pressure. The gaseous phases in the brine were ignored for this example. The cement phase at the beginning of the hydration process was assumed to be fully saturated with water. The effects of both hydration (hardening of the initial cement powder with water) and carbonation (degradation of the calcium-bearing phases in the cement by CO_2) were considered during the evolution of microstructure. To this end, the porosity was calculated through Eq. (2) which is based on solid dissolutions and precipitations. Based on the molar volumes of different cement phases and water-to-cement ratio, the initial porosity is obtained as 0.49. The dissolution kinetics included: (1) hydration (which was considered through specific empirical relationships that are discussed briefly in the following section) and (2) carbonation (which is a result of CO_2 dissolution in cement pore solution and reaction with calcium in the cement paste). The kinetics of hydration and carbonation were assumed to be independent from each other. The required dissolution and precipitation parameters for Eq. (11) were used based on Table 3.

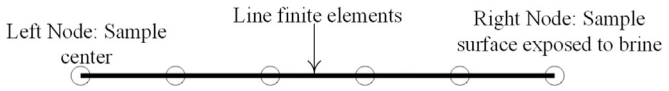

Fig. 7. Domain of the FEM model (noes are for illustration purposes only).

A one-dimensional domain, as shown in Fig. 7, was used to simulate the reactive-transport processes within autoclaved prisms of the experimental part of this investigation with the following assumptions: (1) analysis domain represents a cross section away from the ends of the prism; (2) line of analysis is far from the edges of the prisms; and (3) line of analysis is normal to the sample surfaces. The total length of the domain was equal to half of the sample cross sectional length. The left and right nodes in the geometry show the sample center and exposed surface to the brine, respectively.

To capture the variabilities in the results with initially very low alteration depths, a trial and error approach was used for the element sizes for the domain. Typically 50–100 three-noded Lagrangian finite elements were used to discretize the domain.

The unhydrated cement and brine composition at 23 °C and 0.1 MPa, as given in Tables 2 and 3, were used as initial conditions for the domain. Variable boundary conditions were considered at the brine-cement interface depending on the brine composition, temperature and pressure. Moreover, the changes in brine composition during the analysis were modeled in GEMS3K at each time step. The boundary conditions for the example model include the following steps: (1) pure water exposure in the first 24 hours with 23 °C and atmospheric pressure; and (2) Mt. Simon brine exposure in the next 27 days with increasing pressure and temperature; (3) CO_2 addition to the maximum solubility in the Mt. Simon brine achieving high pressure and high temperature conditions within six hours (i.e. 85 °C and 30 MPa); and (4) continued exposure to high pressure and high temperature conditions for 42 days.

Two analysis cases were considered: (a) high temperature (85 °C) and atmospheric pressure (0.1 MPa) conditions and (b) high temperature (85 °C) and high pressure (28.9 MPa) conditions. The first case was not studied experimentally, but it is included here to demonstrate the effect of pressure on the reactive-transport process. The second analysis case (high pressure and temperature scenario) is compared with available experimental data (Ideker et al., 2014). In both cases the increase in temperature and pressure in the brine is assumed to be achieved within six hours after the cement prisms were exposed to the simulated brine. Typically, the important parameters for degradation of cement include solid volumetric amounts, porosity, and pH profiles under supercritical CO_2 conditions. The dissociation of CO_2 results in the dissolution of portlandite and its replacement with calcite, which reduces the porosity of the medium that causes reduction in CO_2 penetration rate. C–S–H reacts with free H^+ resulting in amorphous silica and in-situ calcite precipitation. Increased concentrations of carbonic acid results in a decrease of pH (6–7), which causes calcite dissolution and, therefore porosity increases, leads to the increased penetration of dissolved CO_2 into the cement and increased alteration depth. The alteration depths in the results are measured from the portlandite dissolution zone to the fully altered region, where all solid phases are dissolved and just amorphous silica is left (brine exposed surface).

Fig. 8 shows the hydrated solid amounts in cement in the beginning of CO_2 exposure at 85 °C and 0.1 MPa pressure (shown as 0 days) and after 42 days of exposure in the same conditions. For consistency, all plots for solid mole amounts are shown scaled to initial phases according to Table 1. For all results, C–S–H shows the sum of a 4-pole model including jennite-D, jennite-H, tobermorite-D and tobermorite-H as obtained from the reaction module at

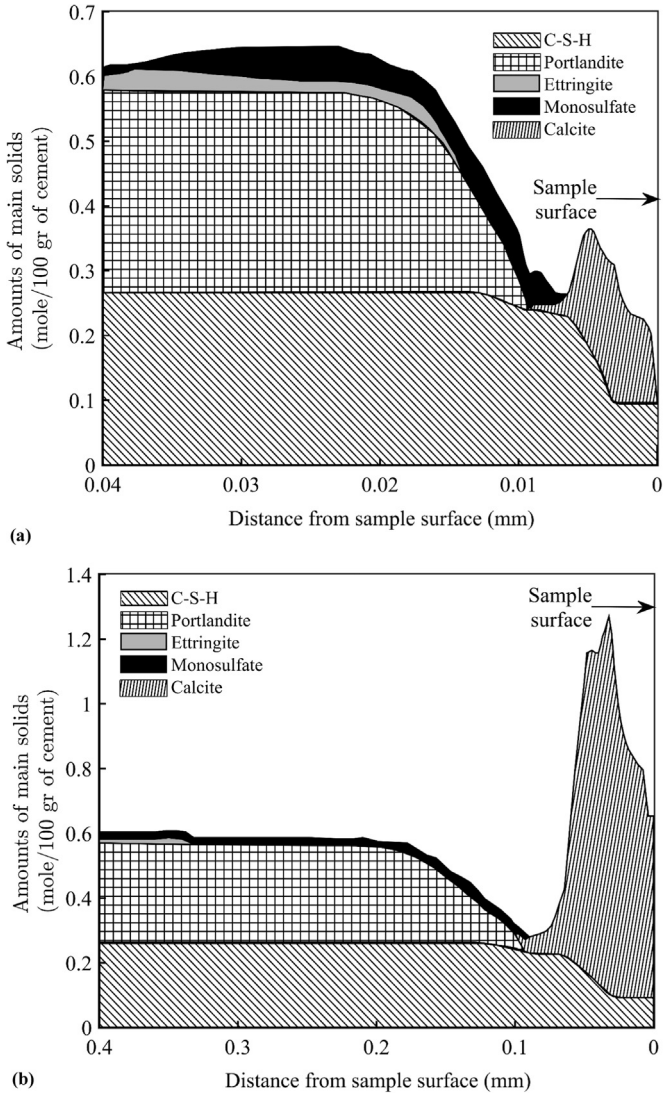

Fig. 8. Solid phases at different ages of CO_2 exposure (T=85°C, atmosphere pressure): (a) At the beginning of the exposure (0 days); (b) after 42 days of exposure. The approximate alteration depth is shown for each case. The domain sizes were assumed differently as 0.04 mm and 0.4 mm for the analyses in (a) and (b), respectively.

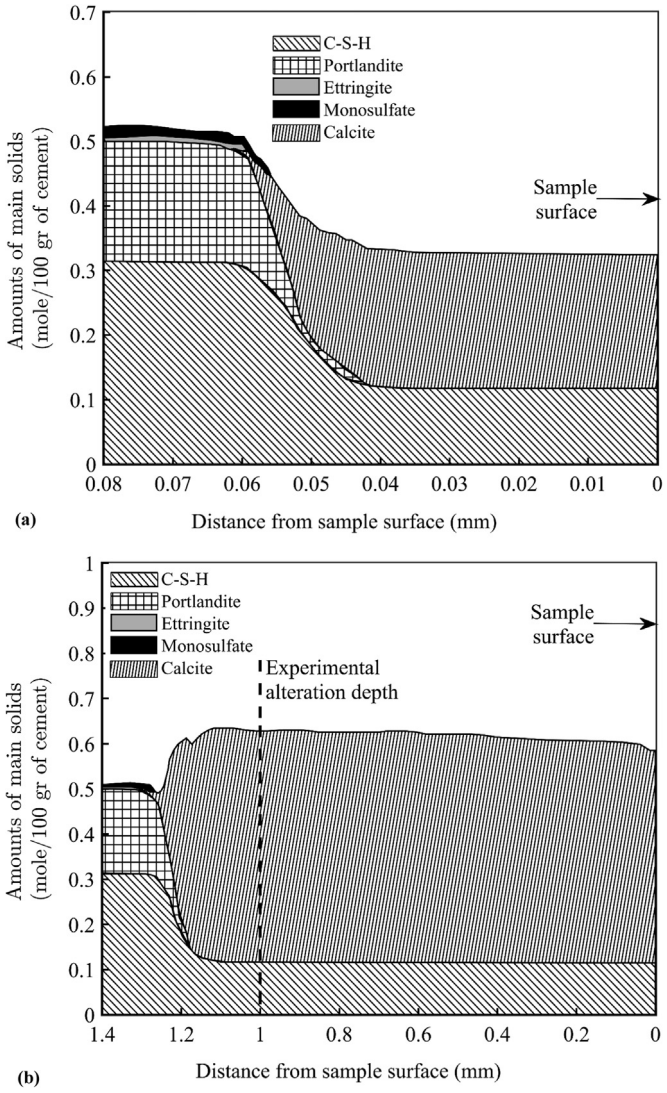

Fig. 9. Solid phases at different ages of CO_2 exposure (T=85°C, P=28.9 MPa): (a) At the beginning of the exposure (0 days); (b) after 14 days of exposure. The approximate alteration depth is shown for each case. The domain sizes were assumed differently as 0.08 mm and 1.5 mm for the analyses in (a) and (b), respectively.

each step of the analysis. Similarly, the monosulfate and ettringite are obtained as the sum of their different types (e.g. Fe-ettringite and Al-ettringite). Fig. 8a shows small alteration depths (about 0.02×10^{-3} m) just before CO_2 exposure starts due to sodium bicarbonate ($NaHCO_3$) present in the Mt. Simon brine. After CO_2 exposure starts, the precipitation of calcite causes a slightly lower porosity near the surface because of a higher molar volume of calcite compared to portlandite. Furthermore, the calcium leaching rate is generally small because of low concentration gradients due to high amounts of calcium in the synthesized brine. The thin calcite front moves into the sample as shown in Fig. 8b after 42 days.

Fig. 9 shows the hydrated solid amounts in cement at the beginning of (0 days) and after 42 days of exposure to CO_2-saturated Mt. Simon brine at 85 °C and at 28.9 MPa pressure. The CO_2 solubility in high pressures is much higher leading to a higher concentration and pressure gradient and consequently higher alteration depths. The alteration depths from this model were compared to those observed from the scanning electron microscope (SEM) micrographs in the parallel experiments.

A comparison between the experimental data and model show slightly greater alteration depths predicted by the COMSOL–GEMS interface model at 14 days (see Fig. 9b) than experimental results. On the other hand, the initial results from the model underestimate the experimental alteration depths. Although these small differences are within the acceptable range of modeling assumptions (e.g. porosity model and diffusion coefficients) and variability in the SEM micrographs, the difference at initial times is likely from the effects of supercritical CO_2 in high pressures, which is ignored in the present model. In fact, the concentration gradient is initially high because of gaseous carbon dioxide in the brine, and it becomes smaller after alteration. The change in pH and porosity are indicative of the vulnerability of the cement in acidic media. The porosity and pH profiles in Fig. 10 show a dense calcite front and low porosity where calcium has leached from the cement in contact with the bulk fluid. Adjacent to the calcite layer, the pH goes down to ~6.8. A small peak in Fig. 10b demonstrates the zone where portlandite has started dissolution and calcite has not precipitated yet.

5. Conclusions

A Java interface was developed for coupling COMSOL API and

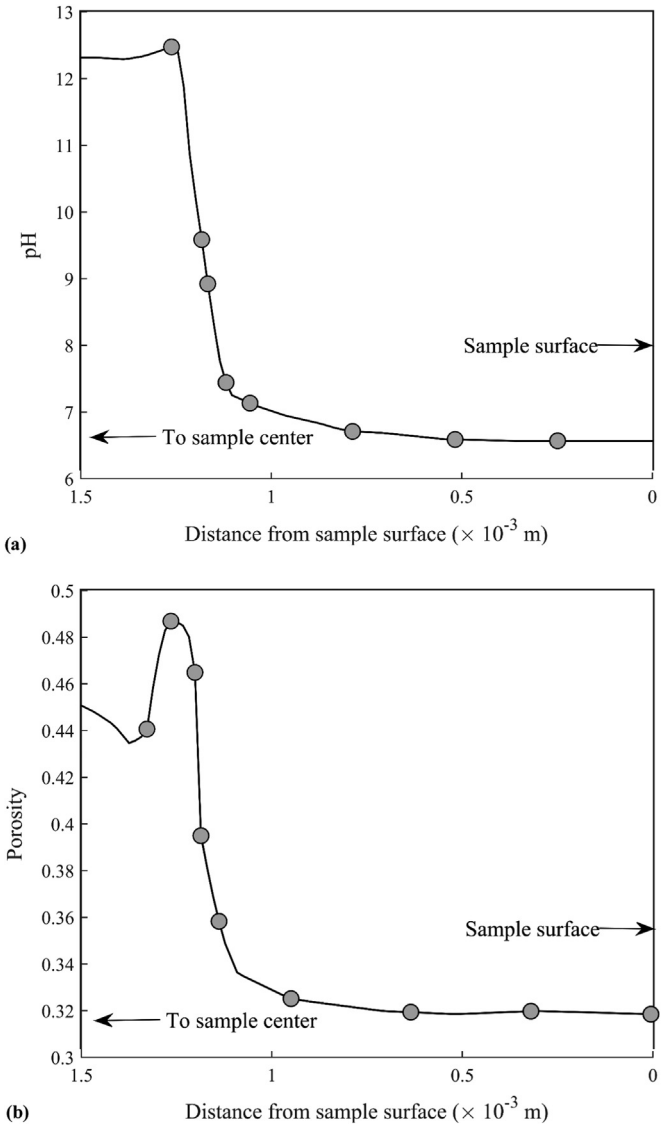

Fig. 10. (a) pH and (b) porosity along cement domain at 42 days of CO_2 exposure (T=85°C, P=28.9 MPa). The average unaltered porosity value was obtained approximately as 0.45 after 42 days of exposure (see left axis).

GEMS3K for the modeling of (geo)chemical coupled reactive-transport processes. The transport equations are fully coupled with potential and fluid flow equations in COMSOL API while they are weakly integrated with the reaction module, GEMS3K, using an operator-splitting technique. The use of a generic finite element software (i.e., COMSOL) allows the inclusion of additional coupled multiphysics phenomena to the problem (e.g. multi-phase flow), and gives users access to inherent mesh generation/refinement, nonlinear solution algorithms and post-processing features. In addition to the advantages of GEM method for analyzing complex (geo)chemical systems, the developed interface can use special thermodynamic databases, developed for GEMS (e.g. CEMDATA) for a large temperature range (0–100 °C).

Acknowledgments

This work was completed as part of National Energy Technology Laboratory (NETL) research for the Department of Energy's Pacific Coast Carbon Storage Initiative. The study was supported by the DOE Office of Fossil Energy, (Grant no. RES1100426/014), under the Office of Oil and Natural Gas (Energy Policy Act of 2005, Section 999 Complementary Program Research).

Appendix A. Supporting information

Supplementary data associated with this article can be found in the online version at http://dx.doi.org/10.1016/j.cageo.2016.04.002.

References

Bary, B., Sellier, A., 2004. Coupled moisture—carbon dioxide–calcium transfer model for carbonation of concrete. Cem. Concr. Res. 34, 1859–1872.
Bažant, Z., Najjar, L., 1972. Nonlinear water diffusion in nonsaturated concrete. Matér. Constr. 5, 3–20.
Bedient, P.B., Rifai, H.S., Newell, C.J., 1994. Ground Water Contamination: Transport and Remediation, 2nd ed. Prentice Hall, New Jersey, USA.
Bethke, C., 1996. Geochemical Reaction Modeling: Concepts and Applications. Oxford University Press, UK.
Boettcher, N., Wang, W., Kolditz, O., Goerke, U.-J., Zehner, B., 2014. Parallel numerical modeling of two-phase flow process in porous medium. In: Proceedings of the 11th international conference on Hydroinformatics, New York, USA.
Ciavatta, L., 1980. The specific interaction theory in evaluating ionic equilibria. Ann. Chim. 70, 551–562.
Comsol, 2013. Comsol Multiphysics, The Platform for Physics-Based Modeling and Simulation, 4 ed. Comsol Inc, Burlington, MA, USA.
Engesgaard, P., Kipp, K.L., 1992. A geochemical transport model for redox-controlled movement of mineral fronts in groundwater flow systems: a case of nitrate removal by oxidation of pyrite. Water Resour. Res. 28, 2829–2843.
Eriksson, G., Hack, K., Petersen, S., 1997. ChemApp—a programmable thermodynamic calculation interface. Werkst. Woche 96, 47–51.
Gasda, S.E., Bachu, S., Celia, M.A., 2004. Spatial characterization of the location of potentially leaky wells penetrating a deep saline aquifer in a mature sedimentary basin. Environ. Geol. 46, 707–720.
Glasser, F.P., Marchand, J., Samson, E., 2008. Durability of concrete—degradation phenomena involving detrimental chemical reactions. Cem. Concr. Res. 38, 226–246.
Guggenheim, E., Turgeon, J., 1955. Specific interaction of ions. Trans. Faraday Soc. 51, 747–761.
Heide, K., 1986. VJ Babushkin, GM Matveyev, OP Mchedlov-Petrossyan. Thermodynamics of Silicates. Springer-Verlag, Berlin, Heidelberg, New York, Tokyo 1985, 459 Selten, 93 Abbildungen, 135 Tabellen, 250,—DM ISBN 3-540-12750-X. Crystal Research and Technology 21, pp. 8–8.
Huet, B.M., Prevost, J.H., Scherer, G.W., 2010. Quantitative reactive transport modeling of Portland cement in CO_2-saturated water. Int. J. Greenh. Gas Control 4, 561–574.
Hummel, W., Berner, U., Curti, E., Pearson, F., Thoenen, T., 2002. Nagra/PSI chemical thermodynamic data base 01/01. Radiochim. Acta 90, 805–813.
Ideker, J.H., Isgor, O.B., Li, C., Jafari, V., Verba, C., Rodriguez, D.E., 2014. Experimental and numerical modeling approach to elucidating damage mechanisms in cement-well casing-host rock settings for underground storage of CO2, NETL-TRS-X-2014, NETL Technical Report Series, U.S. Department of Energy, National Energy Technology Laboratory, Albany, OR, USA, 108 pp.
Johnson, J.W., Nitao, J.J., Knauss, K.G., 2004. Reactive transport modeling of CO_2 storage in saline aquifers to elucidate fundamental processes, trapping mechanisms and sequestration partitioning. Geol. Storage Carbon Dioxide 233, 107–128.
Johnson, J.W., Oelkers, E.H., Helgeson, H.C., 1992. SUPCRT92: a software package for calculating the standard molal thermodynamic properties of minerals, gases, aqueous species, and reactions from 1 to 5000 bar and 0 to 1000 C. Comput. Geosci. 18, 899–947.
Kolditz, O., Bauer, S., Bilke, L., Bottcher, N., Delfs, J.O., Fischer, T., Gorke, U.J., Kalbacher, T., Kosakowski, G., McDermott, C.I., Park, C.H., Radu, F., Rink, K., Shao, H.,

Shao, K., Sun, F., Sun, Y.Y., Singh, A.K., Taron, J., Walther, M., Wang, W., Watanabe, N., Wu, Y., Xie, M., Xu, W., Zehner, B., 2012. OpenGeoSys: an open-source initiative for numerical simulation of thermo-hydro-mechanical/chemical (THM/C) processes in porous media. Environ. Earth Sci. 67, 589–599.
Kosakowski, G., Watanabe, N., 2014. OpenGeoSys-Gem: a numerical tool for calculating geochemical and porosity changes in saturated and partially saturated media. Phys. Chem. Earth, Parts A/B/C 70, 138–149.
Kulik, D., Berner, U., Curti, E., 2004. Modelling chemical equilibrium partitioning with the GEMS-PSI code. In: Smith, B., Gschwend, B. (Eds.), PSI Scientific Report 2003 / Volume IV, Nuclear Energy and Safety. Paul Scherrer Institute, Villigen, Switzerland, pp. 109–122.
Kulik, D.A., 2002. Gibbs energy minimization approach to modeling sorption equilibria at the mineral-water interface: thermodynamic relations for multi-site-surface complexation. Am. J. Sci. 302, 227–279.
Kulik, D.A., Wagner, T., Dmytrieva, S.V., Kosakowski, G., Hingerl, F.F., Chudnenko, K. V., Berner, U.R., 2013. GEM-Selektor geochemical modeling package: revised algorithm and GEMS3K numerical kernel for coupled simulation codes. Comput. Geosci. 17, 1–24.
Lasaga, A.C., 1980. The kinetic treatment of geochemical cycles. Geochim. Cosmochim. Acta 44, 815–828.
Lasaga, A.C., 1984. Chemical-kinetics of water–rock interactions. J. Geophys. Res. 89, 4009–4025.
Leal, A.M., Blunt, M.J., LaForce, T.C., 2013. A robust and efficient numerical method for multiphase equilibrium calculations: application to CO_2–brine–rock systems at high temperatures, pressures and salinities. Adv. Water Resour. 62, 409–430.
Leal, A.M., Blunt, M.J., LaForce, T.C., 2015. A chemical kinetics algorithm for geochemical modelling. Appl. Geochem. 55, 46–61.
Lothenbach, B., Matschei, T., Moschner, G., Glasser, F.P., 2008. Thermodynamic modelling of the effect of temperature on the hydration and porosity of Portland cement. Cem. Concr. Res. 38, 1–18.
Lothenbach, B., Winnefeld, F., 2006. Thermodynamic modelling of the hydration of Portland cement. Cem. Concr. Res. 36, 209–226.
Luckner, L., Van Genuchten, M.T., Nielsen, D., 1989. A consistent set of parametric models for the two-phase flow of immiscible fluids in the subsurface. Water Resour. Res. 25, 2187–2193.
Mainguy, M., Tognazzi, C., Torrenti, J.M., Adenot, F., 2000. Modelling of leaching in pure cement paste and mortar. Cem. Concr. Res. 30, 83–90.
Marty, N.C., Bildstein, O., Blanc, P., Claret, F., Cochepin, B., Gaucher, E.C., Jacques, D., Lartigue, J.-E., Liu, S., Mayer, K.U., 2015a. Benchmarks for multicomponent reactive transport across a cement/clay interface. Comput. Geosci., 1–19.
Marty, N.C., Claret, F., Lassin, A., Tremosa, J., Blanc, P., Madé, B., Giffaut, E., Cochepin, B., Tournassat, C., 2015b. A database of dissolution and precipitation rates for clay-rocks minerals. Appl. Geochem. 55, 108–118.
Marty, N.C., Munier, I., Gaucher, E.C., Tournassat, C., Gaboreau, S., Vong, C.Q., Giffaut, E., Cochepin, B., Claret, F., 2014. Simulation of cement/clay interactions: feedback on the increasing complexity of modelling strategies. Transp. Porous Media 104, 385–405.
Matschei, T., Lothenbach, B., Glasser, F.P., 2007. Thermodynamic properties of Portland cement hydrates in the system $CaO–Al_2O_3–SiO_2–CaSO_4–CaCO_3–H_2O$. Cem. Concr. Res. 37, 1379–1410.
Mayer, K.U., Frind, E.O., Blowes, D.W., 2002. Multicomponent reactive transport modeling in variably saturated porous media using a generalized formulation for kinetically controlled reactions. Water Resour. Res. 38, 13–11-13-21.
Meeussen, J.C., 2003. ORCHESTRA: an object-oriented framework for implementing chemical equilibrium models. Environ. Sci. Technol. 37, 1175–1182.
Moschner, G., Lothenbach, B., Rose, J., Ulrich, A., Figi, R., Kretzschmar, R., 2008. Solubility of Fe-ettringite $(Ca_6[Fe(OH)_6]_2(SO_4)_3.26H_2O$. Geochim. Cosmochim. Acta 72, 1–18.
Nardi, A., Idiart, A., Trinchero, P., de Vries, L.M., Molinero, J., 2014. Interface Comsol-PHREEQC (iCP), an efficient numerical framework for the solution of coupled multiphysics and geochemistry. Comput. Geosci. 69, 10–21.
Palandri, J.L., Kharaka, Y.K., 2004. A compilation of rate parameters of water–mineral interaction kinetics for application to geochemical modeling. DTIC Document.
Parkhurst, D.L., Appelo, C., 1999. User's guide to PHREEQC (Version 2): A computer program for speciation, batch-reaction, one-dimensional transport, and inverse geochemical calculations.
Parrot, L., Killoh, D., 1984. Prediction of cement hydration. Proc. Br. Ceram. Soc., 41.
Paul Scherrer Institute, P., 2013. GEMS: Gibbs Energy Minimization Software for Geochemical Modeling.
Pitzer, K.S., 1991. Activity Coefficients in Electrolyte Solutions. CRC press, Boca Raton, FL, USA.
Prevost, J.H., 1981. DYNA-FLOW: a nonlinear transient finite element analysis program. Princeton University, Department of Civil Engineering, School of Engineering and Applied Science.
Pruess, K., Xu, T., Apps, J., Garcia, J., 2001. Numerical modeling of aquifer disposal of CO_2. In: Proceedings of the SPE/EPA/DOE Exploration and Production Environmental Conference. Society of Petroleum Engineers.
Richards, L.A., 1931. Capillary conduction of liquids through porous mediums. J. Appl. Phys. 1, 318–333.
Shao, H., Dmytrieva, S.V., Kolditz, O., Kulik, D.A., Pfingsten, W., Kosakowski, G., 2009. Modeling reactive transport in non-ideal aqueous–solid solution system. Appl. Geochem. 24, 1287–1300.
Shen, J.Y., Dangla, P., Thiery, M., 2013. Reactive transport modeling of CO_2 through cementitious materials under CO_2 geological storage conditions. Int. J. Greenh. Gas Control 18, 75–87.
Steefel, C., 2009. CrunchFlow Software for Modeling Multicomponent Reactive Flow and Transport. User's Manual. Earth Sciences Division. Lawrence Berkeley, National Laboratory, Berkeley, CA, pp. 12–91.
Steefel, C., Yabusaki, S., 1996. OS3D/GIMRT, Software for Multicomponent-multidimensional Reactive Transport, User Manual And Programmer's Guide. PNL-11166. Pacific Northwest National Laboratory, Richland, Washington.
Steefel, C.I., Lasaga, A.C., 1994. A coupled model for transport of multiple chemical-species and kinetic precipitation dissolution reactions with application to reactive flow in single-phase hydrothermal systems. Am. J. Sci. 294, 529–592.
Thiery, M., 2006. Modélisation de la carbonatation atmosphérique des matériaux cimentaires(prise en compte des effets cinétiques et des modifications microstructurales et hydriques). Etudes et recherches des Laboratoires des ponts et chaussées. Série Ouvrages d'art.
Van der Lee, J., 1998. Thermodynamic and mathematical concepts of CHESS. Technical Report LHM/RD/98/39, ENSMP, Paris, France, 103 pp.
Van Der Lee, J., De Windt, L., Lagneau, V., Goblet, P., 2002. Presentation and application of the reactive transport code HYTEC. Dev. Water Sci. 47, 599–606.
Van Der Lee, J., De Windt, L., Lagneau, V., Goblet, P., 2003. Module-oriented modeling of reactive transport with HYTEC. Comput. Geosci. 29, 265–275.
Van der Lee, J., Lagneau, V., 2004. Rigorous methods for reactive transport in unsaturated porous medium coupled with chemistry and variable porosity. Dev. Water Sci. 55, 861–868.
Van Genuchten, M.T., 1980. A closed-form equation for predicting the hydraulic conductivity of unsaturated soils. Soil Sci. Soc. Am. J. 44, 892–898.
Voss, C.I., 1984. A Finite-Element Simulation Model for Saturated-unsaturated, Fluid-Density-Dependent Ground-Water Flow with Energy Transport or Chemically-Reactive Single-Species Solute Transport. US Geological Survey, Reston, VA, USA.
Wagner, T., Kulik, D.A., Hingerl, F.F., Dmytrieva, S.V., 2012. GEM-SELEKTOR geochemical modeling package: TSolMod library and data interface for multicomponent phase models. Can. Mineral. 50, 1173–1195.
Weast, R.C., Astle, M.J., Beyer, W.H., 1985. CRC Habdbook of Chemistry and Physics. Boca Raton, FL, USA.
Westall, J.C., Zachary, J.L., Morel, F.M., 1976. MINEQL: A computer program for the calculation of chemical equilibrium composition of aqueous systems. Water Quality Laboratory, Ralph M. Parsons Laboratory for Water Resources and Environmental Engineering [sic], Department of Civil Engineering, Massachusetts Institute of Technology.
Wissmeier, L., Barry, D., 2009. Simulation Tool for Variably Saturated Flow with Comprehensive Geochemical Reactions in 2D and 3D Coupling COMSOL Multiphysics® and PHREEQC, Eos Trans. AGU, 90 (52), Fall Meet. Suppl., Abstract H11B-0793.
Xu, T., Spycher, N., Sonnenthal, E., Zhang, G., Zheng, L., Pruess, K., 2011. TOUGHREACT Version 2.0: a simulator for subsurface reactive transport under non-isothermal multiphase flow conditions. Comput. Geosci. 37, 763–774.
Xu, T.F., Sonnenthal, E., Spycher, N., Pruess, K., 2006. TOUGHREACT - a simulation program for non-isothermal multiphase reactive geochemical transport in variably saturated geologic media: applications to geothermal injectivity and CO_2 geological sequestration. Comput. Geosci. 32, 145–165.